Crystalline structure and microstructure of synthetic hexagonal magnesium-cobalt cordierite solid solutions ($Mg_{2-2x}Co_{2x}$ $Al_4Si_5O_{18}$)

Supplementary Material

Francisco Javier Serrano,[a] Noemí Montoya,[b] José Luis Pizarro,[c] María Mercedes Reventós,[a] Marek Andrzej Kojdecki,[d*] José María Amigó[a] and Javier Alarcón[b]

[a]Department of Geology, University of Valencia, 46100 Burjasot , Spain, [b]Department of Inorganic Chemistry, University of Valencia, 46100 Burjasot, Spain, [c]Department of Mineralogy and Petrology, University of the Basque Country, 48080 Bilbao, Spain, and [d]Institute of Mathematics and Cryptology, Military University of Technology, 00-908 Warsaw, Poland. E-mail: m_kojdecki@poczta.onet.pl

Abstract Co^{+2}-containing cordierite glasses, of nominal compositions $(Mg_{1-x}Co_x)_2$ $Al_4Si_5O_{18}$ (with x = 0, 0.2, 0.4, 0.6, 0.8 and 1) were prepared by melting colloidal gel precursors. After isothermal heating at 1273 K and around 28 h, a single-phase a-cordierite (high-temperature hexagonal polymorph) was synthesised. All materials were investigated using X-ray powder diffraction and field-emission scanning electron microscopy. The crystalline structure and microstructure were determined from X-ray diffraction patterns. Rietveld refinement confirmed the formation of magnesium-cobalt cordierite solid solutions. The unit-cell volume increased with the increase of cobalt content in starting glass. The crystalline microstructure of the cordierites was interpreted with using a mathematical model of a polycrystalline material and characterised by prevalent crystallite shape, volume-weighted crystallite size distribution and second-order crystalline lattice strain distribution. Hexagonal prism was the prevalent shape of a-cordierite crystallites. Bimodality in the size distribution was observed and interpreted as a consequence of two paths of the crystallisation: the nucleation from glass of μ-cordierite which transformed into a-cordierite with annealing or the nucleation of a-cordierite directly from glass at high temperature. Scanning electron microscopy images agreed well with crystalline microstructure characteristics determined from the X-ray diffraction line profile analysis.

Keywords: cordierite; crystalline microstructure; volume-weighted crystallite size distribution; second-order crystalline lattice strain distribution; crystallite shape; glass; Rietveld analysis; X-ray diffraction line profile analysis; powder X-ray diffraction pattern modelling

Table S1. Atomic parameters for hexagonal cordierite solid solutions with nominal compositions $(Mg_{1-x}Co_x)_2Al_4Si_5O_{18}$ i.e. $(Mg_{2-2x}Co_{2x})_M\,(Al_2Si)_{T1}\,(Al_2Si_4)_{T2}\,(O_{12})_{O1}\,(O_6)_{O2}$ (x= 0, 0.2, 0.4, 0.5, 0.6, 0.8 and 1.0).

Atomic coordinates and structural site occupancy		Cordierite specimen						
		C00	C02	C04	C05	C06	C08	C10
(Mg, Co):	x	0.67	0.67	0.67	0.67	0.67	0.67	0.67
	y	0.33	0.33	0.33	0.33	0.33	0.33	0.33
	z	0.25	0.25	0.25	0.25	0.25	0.25	0.25
B isotropic		1.50(10)	2.27(9)	1.51(11)	2.04(14)	1.60(11)	0.79(11)	0.13(7)
(Al, Si1):	x	0.50	0.50	0.50	0.50	0.50	0.50	0.50
	y	0.50	0.50	0.50	0.50	0.50	0.50	0.50
	z	0.25	0.25	0.25	0.25	0.25	0.25	0.25
B isotropic		1.14(8)	2.00(8)	1.62(9)	1.72(11)	1.57(10)	0.73(10)	0.08(9)
(Al2, Si2):	x	0.3706(2)	0.3717(2)	0.3706(3)	0.3707(3)	0.3706(3	0.3684(3)	0.3687(3)
	y	0.2644(3)	0.2638(3)	0.2632(3)	0.2629(4)	0.2634(4)	0.2605(4)	0.2614(4)
	z	0.00	0.00	0.00	0.00	0.00	0.00	0.00
B isotropic		1.13(6)	1.68(6)	1.66(7)	2.02(9)	1.24(8)	0.83(8)	0.11(7)
O1:	x	0.4778(3)	0.4760(3)	0.4765(4)	0.4762(4)	0.4743(4)	0.4742(4)	0.4731(4)
	y	0.3472(3)	0.3445(4)	0.3451(4)	0.3463(5)	0.3448(4)	0.3449(5)	0.3452(4)
	z	0.1422(2)	0.1413(2)	0.1404(2)	0.1413(3)	0.1403(3)	0.1402(3)	0.1409(9)
B isotropic		2.22(8)	2.85(8)	2.56(9)	3.13(12)	2.46(11)	2.09(12)	1.35(11)
O2:	x	0.2273(5)	0.2262(5)	0.2225(6)	0.2218(7)	0.2206(7)	0.2231(8)	0.2221(8)
	y	0.3030(4)	0.3018(4)	0.3016(5)	0.3004(6)	0.3006(6)	0.2992(6)	0.2987(6)
	z	0.00	0.00	0.00)	0.00	0.00	0.00	0.00
B isotropic		3.34(13)	3.56(12)	3.60(14)	4.24(18)	3.86(17)	2.82(18)	1.78(16)
Octahedral site distribution:								
Mg		1.00	0.80	0.61	0.52	0.39	0.22	0.00
Co		0.00	0.20	0.39	0.48	0.61	0.78	1.00
Tetrahedral site distribution:								
Al1		0.69	0.70	0.63	0.69	0.69	0.69	0.70
Si1		0.31	0.30	0.37	0.31	0.31	0.31	0.30
Al2		0.35	0.35	0.36	0.35	0.36	0.37	0.35
Si2		0.65	0.65	0.64	0.65	0.64	0.63	0.65
Oxygen site								
O1		1.00	1.00	1.00	1.00	1.00	1.00	1.00
O2		1.00	1.00	1.00	1.00	1.00	1.00	1.00

SM 1. Model of crystalline microstructure and characterisation of polycrystalline materials

SM 1.1. Statistical description of polycrystalline materials

In this work the crystalline microstructure of polycrystalline materials under study is characterised by means of parameters with immediate physical interpretation. Since a mathematical model describing the crystalline order in a polycrystalline specimen was discussed in detail earlier (Kojdecki, 2004; Kojdecki *et al.*, 2001, 2005, 2007, 2009), only the model constitution is briefly explained.

A polycrystalline sample is interpreted as a statistical population of crystallites, which are assumed to be domains with perfect crystalline order inside, each of them scattering X-rays in a coherent way independently of one another, being separated by small-angle or large-angle boundaries and randomly oriented in space. Each crystallite may form a separate grain or be a mosaic block as a part of a grain. In approximation, crystallites are assumed to have same simple shape, being a prevalent one in reality. Each crystallite is assumed to be constituted by the perfect lattice but of lattice parameters varying from each other; point defects inside crystallites and stacking faults (of less importance in materials with a big unit cell containing many atoms) are omitted. In this way the second-order strain (or incompatibility strain) is considered as homogeneous but in general anisotropic inside an individual crystallite. Consequently, the variation of lattice parameters of the crystallites is characterised by the second-order crystalline lattice strain distribution, which may be interpreted as a density of probability of finding a crystallite in which the interplanar distances differ from those in the reference structure according to an assumed relationship (the reference structure is determined by the parameters averaged over all crystallites). This distribution is assumed to be independent of crystallite size and of crystalline direction (as being statistically isotropic). The sizes of the crystallites are characterised by the volume-weighted crystallite size distribution, which may be interpreted as a density of probability of finding a crystallite of an assumed shape and size, taken with a weight proportional to its volume, in an analysed sample. The size of a crystallite is any of its linear dimensions, while the shape is described by the ratios of its characteristic dimensions (like edge lengths of a prism); either the size or the shape are treated as model parameters. To compare the features of different populations of crystallites (of different prevalent shapes), the standardised crystallite size equal to the cube root of the volume is introduced.

When applied to describing real materials, this model of crystalline microstructure can be interpreted as a simplified statistical representation of more complex physical reality; it was verified favourably in recent studies, also with using other methods for investigating material properties (Kojdecki *et al.*, 2000, 2005, 2007, 2009).

Similar models analysed with different details can be found in works by Wilson (1962, 1963, 1970), by Warren (1969), by Scardi & Leoni (2004), by Armstrong *et al.* (2004) and by Langford *et al.* (1993). Overviews of the models and methods used in this branch of crystallography can be found in the survey by Langford & Louër (1996), in books edited by Snyder, Fiala & Bunge (1999), by Mittemeijer & Scardi (2004) and by Dinnebier & Billinge (2008), and also in articles by Louër (2003) and Leoni *et al.* (2004).

SM 1.2. X-ray diffraction pattern from a model polycrystal and inverse problem

In the approximation of the kinematical theory of X-ray scattering, a diffraction pattern may be interpreted as a sum of individual peaks from many crystallites, particularly in the Bragg-Brentano diffractometer geometry. Because large number of crystallites are illuminated by X-ray beam, an XRD pattern involves averaged statistical characteristics of the crystallite population. The XRD pattern depends implicitly on the microstructure of investigated specimen. The model parameters, characterising a real polycrystalline material, may be recovered from XRD data through describing this dependence and solving the corresponding inverse problem. The computations, which are necessary to determining these parameters, are briefly described below (Kojdecki, 2004; Kojdecki *et al.*, 2000, 2007, 2009).

Firstly, pure line profiles, containing all accessible microstructural information, are extracted from experimental peaks by using standard pattern, representing the instrumental contribution (both after background subtraction), according to formula $g_{hkl} * f_{hkl} = h_{hkl}$ (Wilson, 1963). The pure XRD line profile *f* for each *hkl* reflection, corresponding to the Bragg angle $q_{0,hkl}$, may be obtained as a solution of a convolution integral equation of the first kind:

$$\int_{-s}^{+s} g_{hkl}(s-t)\, f_{hkl}(t)\, dt = h_{hkl}(s) \qquad \text{(S1)}$$

when both the line profiles, *g* from a standard sample (instrumental) and *h* from an investigated sample (experimental), are known; *s* is the reciprocal lattice vector length, $s \approx 4p\, l^{-1}(q - q_{0,hkl})\cos q_{0,hkl}$, l is the X-ray wavelength and s is a sufficiently large number.

In the vicinity of the Bragg angle, the pure XRD line profile *f* (for the *hkl* reflection) from a crystal like that described above (particularly consisted of crystallites with the same shape), with a volume-weighted crystallite size distribution *v* and a second-order crystalline lattice strain distribution *r*, may be interpreted (up to an approximately constant multiplier) as

$$\int_{-s}^{+s} \left[\int_0^N Y_{hkl}(n, s-t)\, v(n)\, dn \right] r_{hkl}(t)\, dt = f_{hkl}(s) \qquad \text{(S2)}$$

(Wilson, 1963; Kojdecki & Mielcarek, 2000; Kojdecki, 2004) under the assumption that the structure factor is constant for all crystallites. For assumed crystallite shape and fixed *n* a function $Y_{hkl}(n,s) = n^{-3} F_{hkl}(n,s)$ describes the pure diffraction line (*hkl* reflection) from a single crystallite (scattering X-rays coherently) with a perfect lattice and with a size characterised by a number *n* (taken with weight n^{-3} inversely proportional to crystallite volume); *N* must be sufficiently large (so that $v(n) = 0$ for $n > N$, in a good approximation). Thus the pure line profile may be treated as the convolution $k_{hkl} * r_{hkl} = f_{hkl}$ of two hypothetic lines (functions),

$$\int_{-s}^{+s} k_{hkl}(s-t)\, r_{hkl}(t)\, dt = f_{hkl}(s)\,, \qquad \text{(S3)}$$

one, k_{hkl}, originating only from the shape and size distribution of the crystallites,

$$k_{hkl}(s) = \int_0^N Y_{hkl}(n,s)\, v(n)\, dn\,, \qquad \text{(S4)}$$

and the other, r_{hkl}, originating only from the strain distribution. The function r_{hkl} for each *hkl* reflection may be represented as being equal to the second-order crystalline lattice strain distribution *r* with changed argument:

$$r_{hkl}(q - q_{0,hkl}) = r(-[q - q_{0,hkl}]\cot q_{0,hkl}) \qquad \text{(S5)}$$

which relates to a position shift $q_0 \to q$ of a peak from an individual crystallite. This shift corresponds to the relative change of lattice parameters and interplanar spacings *d*:

$$dd/d \approx -(q - q_0)\cot q_0\,. \qquad \text{(S6)}$$

Crystallites are modelled in the form of a simple convex solid representing well a statistical mean for a sample under study. To materials with hexagonal structure sphere, cylinder with axis of revolution [001], rhombic prism with edges parallel to crystallographic axes (with rhombic base in plane (001)) or hexagonal prism of edges in directions of [100], [010], [110] (of regular hexagonal base in plane (001)) or [001] (other) are applied. A crystallite with shape predominant in an analysed specimen is characterised by a size coefficient n and a shape coefficient k; e.g. a hexagonal prism is defined by the length of largest base diagonal equal to na and height equal to nkc, where a,c are the unit cell parameters.

Each investigated material is characterised by a prevalent crystallite shape, a volume-weighted crystallite size distribution and a second-order crystalline lattice strain distribution, computed from experimental data by simultaneous analysis of several line profiles extracted from XRD patterns. As a criterion of similarity of XRD profiles simulated (with using computed microstructure characteristics) to experimental ones (measured, after subtracting background), the weighted Euclidean norm is applied:

$$R_{wp}(h_{hkl}^{meas}, h_{hkl}^{calc}) \equiv \left[m^{-1} \sum_{hkl} \left\| h_{hkl}^{calc} - h_{hkl}^{meas} \right\|_2^2 \left\| h_{hkl}^{meas} \right\|_2^{-2} \right]^{1/2}, \quad \left\| h_{hkl}^{meas} \right\|_2 \equiv \left[\sum (h_i)^2 \right]^{1/2}. \qquad \text{(S7)}$$

where *m* is the number of simultaneously analysed peaks (included in summation with corresponding indices); peak maximums are treated as free variables. Microstructure characteristics of a sample under study are computed to minimise approximately functional (S7).

Averaged characteristics of a material sample are computed from the size and strain distributions, satisfying usual conditions, $\int_0^{+\infty} v(n)\, dn = 1$ and $\int_{-\infty}^{+\infty} r(t)\, dt = 1$, in accordance with statistical interpretation of the model parameters. For example, the size of the mean crystallite representing a population with hexagonal-prism shape (mentioned above) is characterised by the mean greatest base diagonal D (in plane (001)) and the mean height H (in direction [001]):

$$D = a \int_0^{+\infty} n\, v(n)\, dn\,, \qquad H = k\, D c a^{-1} \qquad \text{(S8)}$$

and the mean-absolute second-order strain is equal to the mean deviation of the strain distribution:

$$E = \int_{-\infty}^{+\infty} |t|\, r(t)\, dt\,. \qquad \text{(S9)}$$

These averaged magnitudes are accompanied with the relative standard deviation (variation coefficient) of the size distribution:

$$S = \left\{ \left[\int_0^{+\infty} n^2\, v(n)\, dn \right] - \left[\int_0^{+\infty} n\, v(n)\, dn \right]^2 \right\}^{1/2} \left[\int_0^{+\infty} n\, v(n)\, dn \right]^{-1} \quad \text{(S10)}$$

and the relative standard deviation of the strain distribution:

$$Z = \left\{ \left[\int_{-\infty}^{+\infty} t^2\, r(t)\, dt \right] - \left[\int_{-\infty}^{+\infty} t\, r(t)\, dt \right]^2 \right\}^{1/2} \left[\int_{-\infty}^{+\infty} |t|\, r(t)\, dt \right]^{-1}. \quad \text{(S11)}$$

The volume fraction of crystallites of size na from the range $[n_1 a, n_2 a]$, with respect to the specimen total volume, is $\int_{n_1}^{n_2} v(n)\, dn$. Similarly, the volume fraction of crystallites of lattice parameters and interplanar distances in the range $[d_0(1+t_1), d_0(1+t_2)]$ around the averaged value d_0, with respect to the specimen total volume, is $\int_{t_1}^{t_2} r(t)\, dt$ (where $-1 < t_1 < t_2$).

The size distribution determined from experimental data is tested whether can it be well approximated to a bimodal logarithmic-normal (LN) distribution, $v \approx p = c_1 p_1 + c_2 p_2$, of components being densities of LN probability distributions with parameters g_i, w_i:

$$p_i(x) = (x w_i \sqrt{2p})^{-1} \exp\left[-(\ln x - g_i)^2 (2w_i^2)^{-1} \right], \quad \text{(S12)}$$

with the mean $m_i = \exp(g_i + 0.5 w_i^2)$ and the standard deviation $s_i = m_i \left[\exp(w_i^2) - 1 \right]^{1/2}$ ($i = 1$ or $i = 2$). Attributing these components to two different crystallite fractions, one can determine the volume content of each fraction in the specimen total volume, c_i (while $\int_0^{+\infty} p(x)\, dx = c_1 + c_2 = 1$). An unimodal LN distribution is included into this model by admitting $c_1 = 1,\ c_2 = 0$.

The strain distribution determined from experimental data is tested whether it can be well approximated by an even function (with the mean value equal to zero) with positive parameters *y* (a multiplier scaling the function integral to unity), *z* and *w*: Pearson's curve of type II

$$W: \quad p(t) = y \left[\max\left\{ 0, (1 - t^2 z^{-2}) \right\} \right]^w \quad \text{(S13)}$$

or Pearson's curve of type VII

$$D: \quad p(t) = y \left[(1 + t^2 z^{-2})^w \right]^{-1}. \quad \text{(S14)}$$

Table S2. (a) The errors $R_{wp}(f, k*r)$ and $R_{wp}(h, g*k*r)$ of best approximation of the system of nine analysed pure line profiles *f* determined from XRD patterns and experimental line profiles *h* by the lines $k*r$ and $g*k*r$ simulated for the model polycrystalline material with the refined parameters [calculated from formula (S7)] resulting from computation involving hexagonal-prismatic model of crystallites. For comparison the errors $R_{wp}(h, g*k*r)$ resulting from computations involving cylindrical or spherical model of crystallites are added. (b) Details of the discrepancies between the experimental *h* and pure *f* line profiles (measured and computed from experimental data) and the corresponding profiles simulated for the model polycrystalline material with the parameters refined for sample C10 ($g*f$, $g*k*r$ and $k*r$).

(a)

	Hexagonal prism		Cylinder	Sphere
Sample	$R_{wp}(f, k*r)$	$R_{wp}(h, g*k*r)$	$R_{wp}(h, g*k*r)$	$R_{wp}(h, g*k*r)$
C00	0.153	0.110	0.110	0.105
C02	0.205	0.125	0.126	0.116
C04	0.210	0.131	0.136	0.130
C05	0.211	0.134	0.136	0.129
C06	0.190	0.130	0.131	0.123
C08	0.204	0.135	0.135	0.138
C10	0.227	0.135	0.142	0.135

(b)

Pure-cobalt cordierite C10			
Peak	$R_{wp}(h, g*f)$	$R_{wp}(f, k*r)$	$R_{wp}(h, g*k*r)$
010	0.027	0.181	0.095
110	0.114	0.236	0.121
012	0.021	0.171	0.119
112	0.019	0.190	0.101
022	0.027	0.214	0.123
121	0.027	0.199	0.129
122	0.040	0.209	0.123
132	0.028	0.230	0.130
224	0.061	0.355	0.261
C10	0.050	0.227	0.135

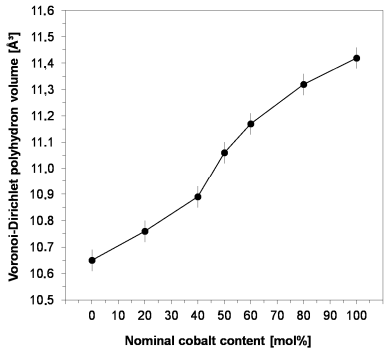

Figure S1. Evolution of the Voronoi-Dirichlet polyhedron volume related with metal octahedral sites for the studied samples.

It can be concluded that the cordierite structure adjusts to Co-Mg substitution in the entire compositional range with the increase of the unit cell volume mainly due to the enlargement of lattice parameter *a*. This is in agreement with the Voronoi-Dirichlet polyhedra (VDP) volume analyses [Blatov *et al.* (1995), Peresypkina & Blatov (2000) , Blatov & Shevchenko (2003), Baburin & Blatov (2004), Blatov (2006)] of the M1, T1 and T2 sites shown in Table 2. The analysis of the T1 and T2 VDP volumes (tetrahedral sites) do not show any trend with the composition of samples. However in the M octahedral sites these VDP volumes increase with the content of Co (Figure SM1), in compatibility with unit cell volume change (Table 1, Figure 4b).

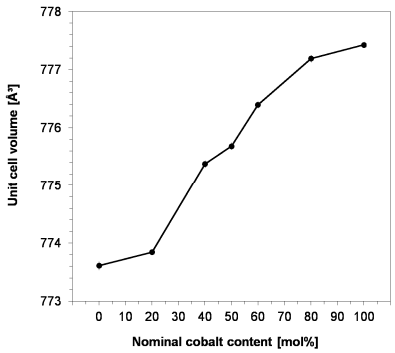

Figure S2. Unit-cell volumes of a-cordierite in dependence on nominal cobalt content. Error bars are within pointers.

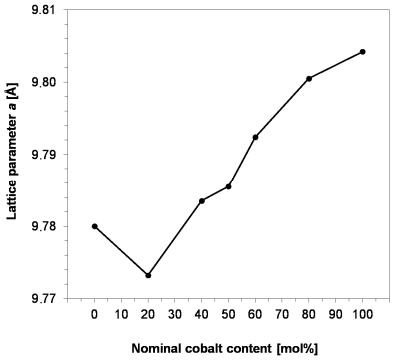

(a)

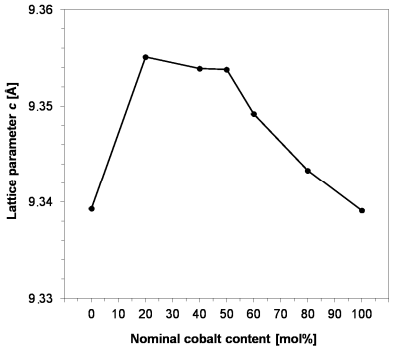

(b)

Figure S3. Hexagonal unit-cell parameters *a* (a) and *c* (b) of a-cordierite, in dependence on nominal cobalt content. Error bars are within pointers.

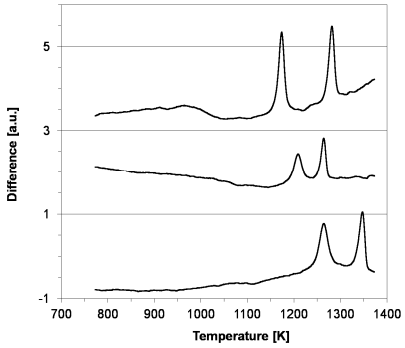

Figure S4. Differential thermal analysis curves registered on heating samples C10 (shifted up a 4 units), C05 (shifted up a 2 units) and C00. Two strong exothermic peaks correspond to formation of μ-cordierite and a-cordierite.

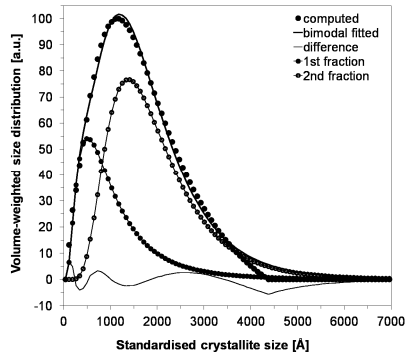

(a)

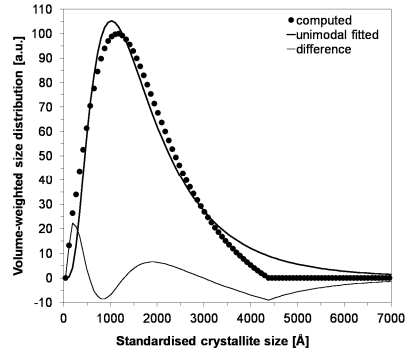

(b)

Figure S5. Example of modelling the volume-weighted standardised crystallite size distribution computed from the XRD data for sample C10 (circles) by (a) a bimodal logarithmic-normal distribution (thick line), with the difference curve (thin line; $R_2 = 0.054$) and both components added (small filled circles and small open circles with thin lines), and by (b) an unimodal logarithmic-normal distribution (with difference curve added; $R_1 = 0.135$). The parameters of these distributions are given in Table 3 and Table 4 of the article.

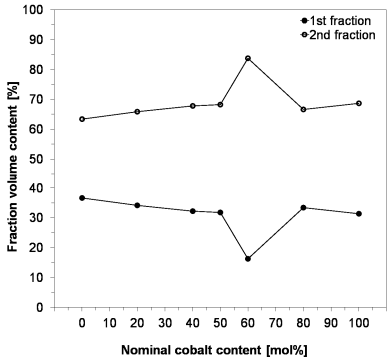

Figure S6. Evolution of volume contents of two fractions of hexagonal-prismatic crystallites in a-cordierites with nominal cobalt content (*cf.* Table 4).

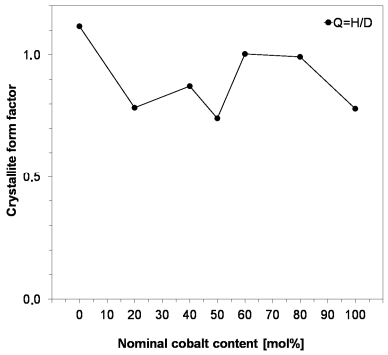

Figure S7. Evolution of shape coefficients (aspect ratios) of hexagonal-prismatic crystallites in magnesium-cobalt a-cordierites with nominal cobalt content ($Q = C/D$, *cf.* Table 3). Roughly, $Q \approx 1.1$ for sample C00, $Q \approx 1$ for samples C06, C08 and $Q \approx 0.8$ for other samples.

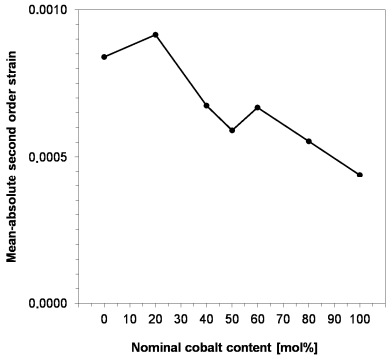

Figure S8. Evolution of mean-absolute second-order strain with cobalt content.

Additional references

Baburin, I. A. & Blatov,V. A. (2004). *Acta Crystallogr.* B**60**, 447-452.

Blatov, V. A., Shevchenko, A. P. & Serezhkin,V. N. (1995). *Acta Crystallogr.* A**51**, 909-916.

Blatov. V. A. & Shevchenko, A. P. (2003). *Acta Crystallogr.* A**59**, 34-44.

Blatov, V. A. (2006). IUCr Comp. Comm. Newslett. **7**, 4-38; http://www.topos.ssu.samara.ru.

Miyashiro, A. & Iiyama, J.T. (1954). *Imp. Acad. Jpn. Proc.* **30**, 746–751.

Miyashiro, A. (1957). *Am. J. Sci.* **255**, 43-62.

Ohsato, H., Kagomiya, I., Terada, M. & Kakimoto, K. (2010). *J. Eur. Ceram. Soc.* **30**, 315–318.

Peresypkina, E. V. & Blatov, V. A. (2000). *Acta Crystallogr.* B**56**, 1035-1045.

Putnis, A. & Bish, D.L. (1983). *Am. Mineral.* **68**, 60-65.

Putnis, A., Salje, E., Redfern, S.A.T., Fyfe, C.A. & Strobl, H. (1987). *Phys. Chem. Miner*. **14**, 446-454.